Investigation of Internal Partitioning in Metallic Enclosures for EMI Control

S. Radu, M. Li, J. Nuebel*, D. M. Hockanson, Y. Ji
J.L.Drewniak, T.H.Hubing, T.P.VanDoren

Electromagnetic Compatibility Laboratory
Department of Electrical Engineering
University of Missouri–Rolla
Rolla, MO 65409-0040

*Electromagnetic Compatibility Group
Sun Microsystems, Inc.
2550 Garcia Avenue
Mountain View, CA 94043-1100

Abstract: High clock frequencies and short edge rates in present high-speed digital systems result in EMI problems at increasingly higher frequencies. At these speeds, clock harmonics have sufficient energy in the range above 500 MHz to excite cavity modes of a conducting enclosure, and to drive even small length slots and apertures that are unavoidable in a practical design, and can result in an EMI problem. One approach to mitigate these problems is to partition the enclosure into several smaller internal shielded compartments. To study the factors which affect this partitioning, a special enclosure that can be divided into two internal compartments using center planes with different types of openings, was designed. The objective is to study the coupling through the center plane for different types and numbers of openings in the center plane and front panel. The experimental results are compared with finite-difference time-domain (FDTD) simulations.

I. INTRODUCTION

A large shielding enclosure is often divided into smaller ones for mechanical reasons, or as a result of a center plane into which PCB modules are plugged, or as internal shielding. As frequencies and edge rates in high-speed digital designs continue to increase, EMI as a result of radiation through slots, apertures, and seams in shielding enclosures is becoming increasingly problematic. There is sufficient energy at low-order clock harmonics to cause EMI problems above a few hundred MHz as a result of exciting cavity modes of the enclosure, and efficiently driving even small length slots and apertures that are unavoidable in a practical design. One possibility for moving cavity resonances beyond the maximum test frequency required by the FCC is to partition the enclosure into smaller internal shielding compartments. Partitioning can serve two purposes. First it can isolate a noise source from electronics in one compartment from an exterior aperture in another that could result in an EMI problem. Second, because the Q of a cavity is proportional to the volume/surface ratio of the cavity [1], each of the smaller cavities will have a smaller Q. The interior circuitry will further reduce the Q.

A Sun S-1000 [1] server was employed for portions of the study. The power supply, CD-ROM, disc drives, and a control card were located in one compartment, and were separated from the main motherboards with CPUs and memories in another by a center plane comprised of a 12-layer PCB fitted into a conducting wall that together spanned the width of the enclosure. The PCB ground layers in the center plane were tied through multiple screws to the chassis. Mechanical and thermal considerations as well as connectors to plug in PCBs necessitated several slots, apertures and holes in the center plane. These penetrations and perforations allow energy to couple between the two internal cavities, and to drive unintentional external slots and apertures on the rear and front panels. For example, in the S-1000, even with the CPU module located in the rear compartment of the enclosure, significant radiation at the CPU clock harmonics was measured through an unintended long slot in the front panel. The CPU clock itself was not routed to the front compartment, but energy was coupled directly through the center plane openings, as well as the signal lines and power bus routed through the backplane between front and rear compartments. However, after an almost complete shielding of the center plane with copper

[1]Sun and S-1000 are registered trademarks of Sun Microsystems Computer Company.

0-7803-4140-6/97/$10.00

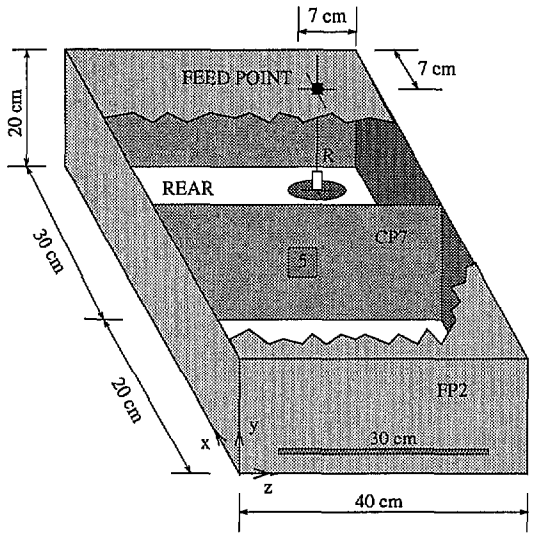

Figure 1. The specially designed enclosure used in this study (not at scale).

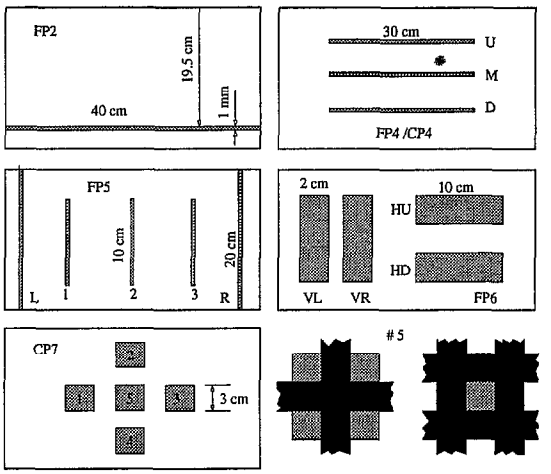

Figure 2. Different front panels (FP) and center planes (CP) used in the experiments and simulations.

tape and fine screen mesh that still allowed for air flow, a significant reduction (> 10 dB over a broad frequency range) in the radiation was measured, indicating significant coupling through the center plane openings that lead to radiated EMI.

II. EXPERIMENTAL STUDY OF A REGULAR ENCLOSURE DESIGN

Energy coupling between compartments in a shielding enclosure as a result of perforations in the interior conducting partition was difficult to study in the functional S-1000 equipment. The basic coupling mechanism is affected by the interior circuitry, uncontrolled common-mode noise sources, unintended coupling paths, and unintentional antennas. To reduce the complexity inherent in the functional S-1000, and to have a controlled environment for investigating the coupling, a special enclosure with approximately the dimensions of the S-1000 (50 $cm \times 40$ $cm \times 20$ cm), shown in Fig.1, was constructed of sheet aluminium. A 20 $cm \times 40$ cm center plane can be inserted 20 cm from the front panel, approximating the position of the center plane in the S-1000. Six versions of the front panel and center plane were designed plus solid planes for reference. Each front/center plane had different types and numbers of openings; e.g., horizontal or vertical slots (0.1 cm width), horizontal or vertical apertures (10 $cm \times 2$ cm), rectangular holes (3 $cm \times 3$ cm), or circular holes ($d = 3.4$ cm). A number of experimental configurations were possible by combining different center planes and front panels as shown in Fig.2, to gain some insight into the coupling physics.

The configuration of the specially designed enclosure was also used for FDTD simulations. To maintain a reasonable time-history in the simulations, the cavity was fed with a wire terminated in a resistor. The power dissipated in the resistor affects the Q of the cavity, thereby reducing the necessary FDTD time history. This was particularly important for modes where appreciable power was not radiated. The feeding point was placed asymmetrical on the top, in a rear corner 7 cm away of each edge, as shown in Fig.1. The enclosure was fed by extending the center conductor of a type-N bulkhead connector to span the enclosure, and was terminated on the opposite wall in a $47.8\ \Omega$ 1206 SMT resistor [2]. This geometry also supported a TEM mode. There is not a closed form expression for the characteristic impedance of a transmission line for the geometry being considered with the feed probe as center conductor and the enclosure walls as outer conductor. The characteristic impedance $Z_0 = 255.8\ \Omega$ was determined experimentally using a Tektronix 11801B Digital Sampling Oscilloscope and TDR.

Two port swept frequency measurements were made in the range 0.3–1.2 GHz using a Wiltron 37247A Network Analyzer. $|S_{21}|$ measurements were conducted in an FACT 3 Lindgren RF shielded anechoic chamber. An Electrometrics LFP-2F log periodic dipole array was used as the receiving antenna. The received signal of the antenna was amplified at Port 2 of the Network Analyzer with an HP 8449B Preamplifier with 35 dB gain above 1 GHz. The thru of the two-port calibration was done without the preamplifier or antenna in path. While the $|S_{11}|$ measurements were calibrated with the reference plane at the cavity feed terminals, the $|S_{21}|$ measurements are relative radiated fields only.

In all the experiments, the distance between EUT and antenna was 3 m, and the front panel with the open aperture or slot was facing the receiving antenna.

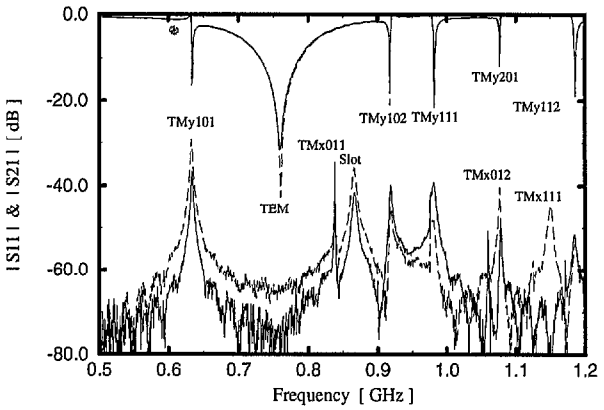

Figure 3. $|S_{11}|$ and $|S_{21}|$ for the front panel FP2 (30 cm) and different openings in the center plane CP7 (solid line: #3, 5; and, long-dashed line: #1, 2, 3, 4, 5 apertures opened).

Selected experimental results are shown in Figs.3–7 that illustrate the essential coupling physics. The cavity where the feeding point is placed is denoted as the rear cavity, and the cavity with the front panel, as the front cavity. The rear cavity is "loaded" by the front cavity through the openings in the center plane, and the Q of a specific cavity mode will be affected by the type of center plane used [3]. However, the cavity resonance frequencies were relatively unaffected by the center plane apertures studied. Ignoring the openings in the center plane and the particular excitation method, the theoretical frequencies for an ideal cavity were approximately those measured [4], [5], with the difference being less than 4% for the frequency range considered. This suggests that the field distribution for a specific mode in the cavity studied was approximately that for an ideal cavity of the same dimensions. The field distributions provide insight into the feed point locations of noise sources, e.g., poorly grounded heatsinks that can result in significant cavity excitation, and into the currents induced on the center plane surface, hence, the critical locations and type for any center plane openings. The excitation of a mode is greatest if the source is located where the field is a maximum. For example, if the source excites predominantly the electric field, a source located at a maximum of the electric field with the polarization oriented in the field direction will lead to maximum excitation. Such sources can include heatsinks or floating metal. Modes can be excited similarly by magnetic-field sources such as current loops. A knowledge of the field distribution inside the cavity is also helpful in placing a lossy material to load the cavity and reduce EMI [6].

The resonance frequencies of the modes of the rear cavity are indicated on the $|S_{11}|$ data in Figs.3–8. Only TM_ynlm modes are excited because of the source type and orientation. The resonance frequencies of the modes in the front cavity are indicated on the $|S_{21}|$ data as TM_xnlm, to clearly distinguish them from the resonances associated with modes of the rear cavity. For clarity in the figures, only one of several degenerate modes is indicated. However, in the front cavity both TM_xnlm and TE_xnlm are possible, and $f(TM_x011) = f(TE_x101) = 0.84\ GHz$, $f(TM_x012) = f(TE_x102) = f(TE_x110) = 1.06\ GHz$, $f(TM_x111) = f(TE_x111) = 1.124\ GHz$ are degenerate modes. For the rear cavity, there are no degenerate modes in the frequency range studied.

The measurements shown in Fig.3 are for two and five 3 cm × 3 cm square holes in the center plane CP7. Significant radiation through the slot in the front panel indicated by the $|S_{21}|$ measurements resulted at all resonance frequencies of the rear cavity. The first three modes of the front cavity are also excited and lead to appreciable radiation through the front panel slot. A resonance occurs at 0.865GHz that is not associated with a cavity mode of either front or rear cavity, and is not an integer $\lambda/2$ resonance of the 30 cm long slot in the front panel (expected at 0.5 GHz and 1.0 GHz), but results from the presence of the slot.

In some cases, the amplitude differed by less than 10 dB for two or five apertures, as shown in Fig.3. Also, the frequency of the resonance at 0.865 GHz resulting from the slot in the front panel is not affected by the number of coupling apertures in CP7. From an EMI perspective, the peaks of the radiation are of interest. However, the radiated field amplitude is a function not only of the location, shape, size and number of apertures in the center plane, but also the source location, geometry and polarization as well as the location, shape, and size of the apertures through which energy is radiated from the front panel. There are potential resonances associated with modes of the rear cavity, front cavity, as well as with the slot in the front panel. The measurements in Fig.3 indicate that appreciable energy is radiated at the resonance frequencies of the rear cavity. The large amplitude fields in the rear cavity at resonance couple sufficient energy through the center plane apertures and front cavity to the front panel slot, though neither the front cavity or slot are resonant. Similarly, energy is coupled from the source in the non-resonant rear cavity through the aperture to result in significant radiation at resonance frequencies of the front cavity. However, within the frequency range studied, the source in the rear cavity did not appreciable excite an $\lambda/2$ resonance in the front panel slot for these coupling apertures studied. In all cases, the square coupling apertures were non-resonant in the studied frequency range.

The configuration studied for the measurements in Fig.4 is similar to that for Fig.3, except a 3 cm × 3 cm square hole is compared with a small 1 cm^2 square aperture and four 1 cm^2 apertures shown in Fig.2. Though the area is 9

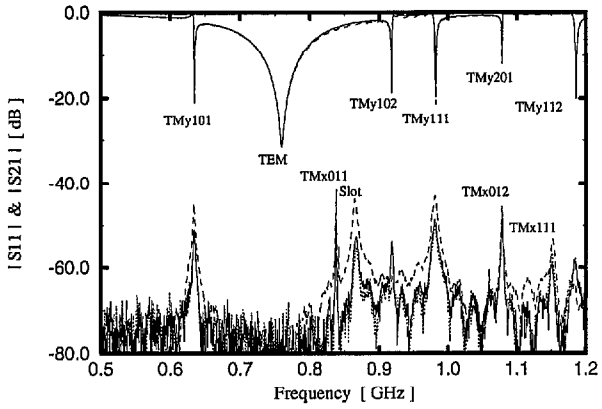

Figure 4. $|S_{11}|$ **and** $|S_{21}|$ **for the front panel FP2 (30** cm**) and different openings in the center plane CP7 (solid line: four squares of 1** cm^2 **each in #5; dotted line: one square of 1** cm^2 **in #5; dashed line: #5).**

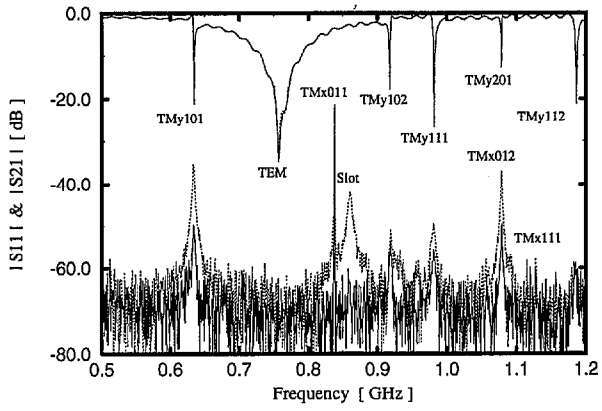

Figure 5. $|S_{11}|$ **and** $|S_{21}|$ **for the front panel FP4M (30** cm **horizontal slot in the middle) and different openings in the center plane CP7 (solid line: one square of 1** cm^2 **in #5; dotted line: # 5).**

times smaller for a single aperture, the radiated field amplitudes differ by typically less than 10 dB, though the levels are affected differently for every mode. Also, the radiated field differs little between a single 1 cm^2 aperture and four 1 cm^2 apertures. To significantly reduce radiation through the front panel slot, the coupling aperture size must be appreciably smaller than 1 cm^2. In partitioning enclosures, perforations and penetrations are required for many reasons including air flow, fan location, connectors, cabling, etc. In the case of apertures, a conducting screen mesh is necessary over these perforations in order to minimize potential EMI problems related to field coupling between cavities. Cost and manufacturing constraints may prohibit this solution, however, the benefits of a compromised partition may be negligible.

$|S_{11}|$ and $|S_{21}|$ results for 1 cm × 1 cm and 3 cm × 3 cm square apertures centered in the center plane are shown in Fig.5. The front panel FP4M has a 30 cm long slot in the middle of the panel. The resonance at 0.865 GHz associated with the slot (though not a $\lambda/2$ resonance) is very clear with the 3 cm × 3 cm aperture in the center plane CP7, but no energy is coupled out the front panel at this frequency for a 1 cm^2 aperture. Also, the radiation at the TM_y101 and TM_y201 mode resonances are significantly reduced for this center plane configuration with a smaller aperture size. The change in the slot position in the front panel has affected the excitation of the slot, and subsequent radiation, however, the radiation still peaks at the resonances of the front and rear cavities. The results shown in Fig.6 are for the same center plane CP7 with one 3 cm×3 cm square aperture, but with different front panels shown in Fig.2. The resonance around 0.865 GHz occurs only for 30 cm long horizontal slots in the front panel FP2

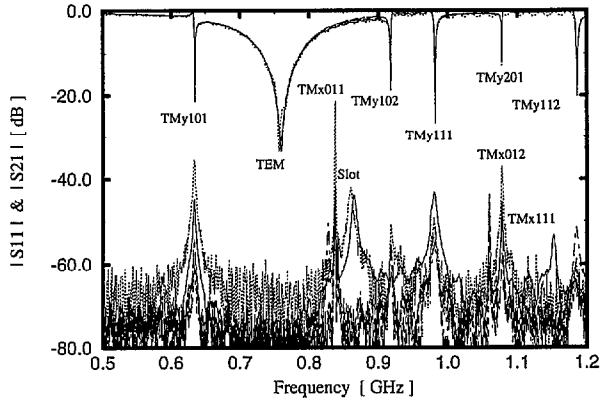

Figure 6. $|S_{11}|$ **and** $|S_{21}$ **for different front panels and #5 opened in the center plane CP7 (solid line: FP2; dotted line: FP4M; dashed line: FP5R; long-dashed line: FP6VL; long-short dashed line: FP6HD)**

or FP4M. The greatest radiation for the cases studied is not for the largest apertures (FP6VL, FP6HD), but for slots on the front panel FP2 and FP4M. The resonance at approximately 0.865 GHz associated with the slots FP2 and FP4M, does not occur for the larger apertures. The resonance around 0.865 GHz does not occur for the vertical slots FP5, but the radiation at the resonances of the front and rear cavities are still present. The vertical slots are less excited, possibly as a result of a TM_{slot} excitation instead a TE_{slot} excitation [7].

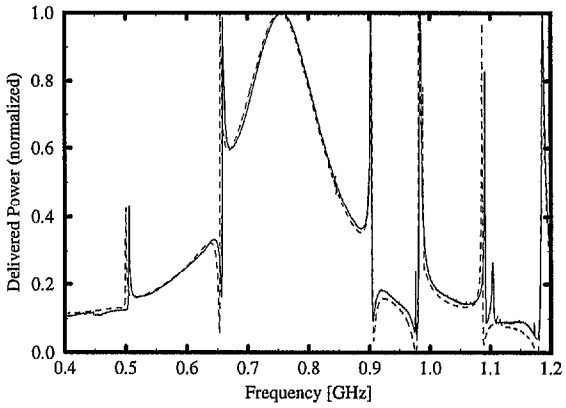

Figure 7. Power delivered to the enclosure calculated from $|S_{11}|$ measurements (solid line) compared with the FDTD simulation (dashed line); center plane CP4M (with a 30 cm long slot in the middle), the front panel FP2 (with a 40 cm long slot in the bottom), with the width 1 mm for both slots, and feed probe termination of 47.8 Ω.

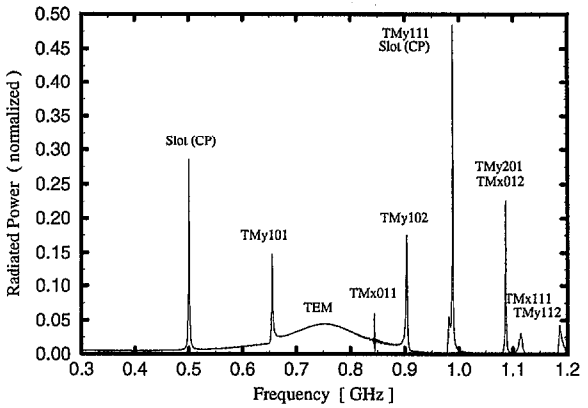

Figure 8. Radiated power, calculated from the FDTD simulations, for the case of Fig.7.

III. FDTD SIMULATION OF COUPLING THROUGH PARTITION APERTURES

It is clear from the measurements presented in the previous section that in a practical design it is difficult to predict coupling and radiated field levels based on simple analytical formulas. However, early direction for developing enclosure design is important in assessing the benefits of partitioning, and the effects of coupling apertures in a partition, as well as estimating radiated EMI levels for approximate source geometries and potential slots or apertures in the exterior enclosure walls. The Finite-Difference Time-Domain (FDTD) method can be a useful numerical approach for pursuing different "what-if" scenarios.

Experimental and FDTD results in the frequency range $0.4 - 1.2\ GHz$ for one specific configuration are shown in Fig.7. The center plane CP4M, as shown in Fig.2, has a slot 30 cm long and 1 mm wide in the middle. The front panel FP2 has a slot 0.5 cm away the bottom edge that is 40 cm long and 1 mm wide. Using simple manipulations of the $|S_{11}|$ data, the delivered power normalized to the available power is presented. For this center plane, there is a clear $\lambda/2$ slot resonance at 0.5 GHz and a λ slot resonance around 1.0 GHz that were not excited in the previous cases with the smaller square coupling apertures. All the expected mode resonances in the driven rear cavity are present, and even the resonances of the front cavity modes can be detected as small discontinuities in $|S_{11}|$. In general, the agreement between the simulations and measurements is good. As a result, the coupled and radiated power can be calculated with some confidence from the FDTD simulations. This is of considerable use in developing enclosure designs since measurements of the absolute radiated power are difficult, and constructing hardware prototypes for pursuing "what-if" scenarios for many iterations is cumbersome. An estimation of the radiated power is shown in Fig.8. In addition to significant radiation at cavity modes, the radiation at resonances of the center plane slot is also appreciable. At the 0.5 GHz center plane slot resonance the radiated power is 28% of the delivered power. The estimation of the radiated power is based on the assumption that the losses in the cavity walls can be neglected, and all the delivered power which is not dissipated in the terminating resistor will be radiated.

The cell size was 1 cm^3 (cubic cell) and the time step was 16.7 ps for this simulation. A total of N=30000 time steps were used but can be reduced using Prony's method [8] or matrix pencil method [9]. The slot in the center plane was modeled with a subcellular capacitive thin-slot formalism [10]. The slot near the corner on the front panel was modeled similarly [11]. Taflove's thin wire algorithm was used for the wire [12] with an effective wire radius of 70% of the physical radius [2]. A sinusoidally modulated Gaussian pulse similar to that in [2] was used for the source. The source and resistive termination were also modeled as in reference [2].

IV. SUMMARY AND CONCLUSIONS

Coupling through apertures in a conducting enclosure with internal partitions was investigated in this paper. The experimental results and simulations presented indicate that even a relatively small aperture can compromise the integrity of a partition, and couple energy through the partition to a perforation in an exterior wall of an adjacent cavity, resulting in significant radiation. Coupling through partition perforations and radiation were significant at all

the rear and front cavity mode resonance frequencies. Energy was coupled and radiated at resonances of either cavity, even for non-resonant lengths of the front panel slot. In the case where a center plane slot is resonant, and/or the resonance frequencies of the cavities are very close, the radiation can be very significant. The frequencies of the cavity resonances were approximately those for an ideal rectangular cavity, even with the apertures and slots loading the cavities.

The physics for coupling through an aperture or slot in an internal partition in a conducting enclosure are currently not well understood. However, the results presented indicate that typical size holes used for air flow can compromise the effectiveness of a partition. In many cases apertures and openings may require a screen mesh to maintain the shielding integrity of the partition.

Experimental design of a shielding enclosure can be arduous and time-consuming. Further, when the enclosure hardware is available in the design cycle, many features of the mechanical design may be determined, such as the location and size of the apertures. FDTD is a viable means for developing and evaluating enclosures designs early. The results presented indicate that FDTD can be used to assess the integrity of a shielding enclosure and potentially to estimate EMI.

Common-mode sources at the PCB level within an enclosure can excite cavity resonances. From a design perspective, harmonics of any system clock can drive these common-mode sources and potentially excite a cavity resonance. However, the experimental results and FDTD simulations presented are a first step in identifying significant aspects and modeling of this problem. Further work is needed for a better understanding of the coupling physics. FDTD can be employed for more realistic modeling of interior irregularities including a number of partitions with perforations, PCB conducting planes, heatsinks, and other large metal structures. However, the effects of a PCB populated with electronics on reducing the Q of resonances needs to be determined experimentally, and approximated in the FDTD modeling. More realistic models for common-mode sources driving the EMI process at the board level are also needed. Once the interior problem is modeled with FDTD, an estimate of EMI for comparison with FCC limits can be made using the FDTD calculated aperture fields for the exterior problem.

V. ACKNOWLEDGMENTS

The authors gratefully acknowledge Sun Microsystems Inc. for access to their anechoic chamber.

REFERENCES

[1] Ramo, S., Whinnery, J. R., Van Duzer, T., *Fields and Waves in Communications Electronics*, John Wiley & Sons, Inc., New York, 1994.

[2] Li, M., Ma, K.-P., Hockanson, D.M., Drewniak, J.L., Hubing, T.H., Van Doren, T.P., "FDTD modeling of thin-slots near corners of shielding enclosures," accepted for publication in *IEEE Transactions on Electromagnetic Compatibility.*

[3] Collin, R. E., *Field Theory of Guided Waves*, IEEE Press, New York, 1991.

[4] Marcuvitz, N., *Waveguide Handbook*, Peter Peregrinus Ltd., London, 1986.

[5] Collin, R. E., *Foundations for Microwave Engineering*, McGraw-Hill, Inc., New York, 1992.

[6] Li, M., Radu, S., Nuebel J., D.M., Drewniak, J.L., Hubing, T.H., Van Doren, T.P., "Reducing EMI through shielding enclosures perforations employing lossy materials: FDTD modeling and experiments," accepted for publication in *Proc. of the 13th ACES Symposium*, Monterey, California, March 17-21, 1997.

[7] Butler, C. M., "A formulation of the finite-length narrow slot or strip equation," *IEEE Transactions on Antennas and Propagation*, vol. AP-30, pp. 1254-1257, November 1982.

[8] Ko, W. L., Mittra, R., "A comparison of FD-TD and Prony's methods for analyzing microwave integrated circuits," *IEEE Trans. Microw. Theory Tech.*, vol. 39, pp. 2176-2181, December 1991.

[9] Sarkar, T. K., Pereira, O., "Using the matrix pencil method to estimate the parameters of a sum of complex exponentials," *IEEE Antennas and Propagation Magazine*, vol. 37, No. 1, pp. 48-55, February 1995.

[10] Gilbert, J, Holland R., "Implementation of thin-slot formalism in the finite-difference EMP code THREDII," in *IEEE Transactions on Nuclear Science*, vol. NS-28, pp.4269-4274, December 1981.

[11] Ma, K.-P., Li, M., Drewniak, J.L., Hubing, T.H., Van Doren, T.P., "A comparison of FDTD algorithms for subcellular modeling slots in shielding enclosures," accepted for publication in *IEEE Transactions on Electromagnetic Compatibility.*

[12] Taflove, A., *Computational Electrodynamics. The Finite-Difference Time-Domain Method*, Artech House, Inc., Norwood, MA, 1995.